ICSV14
Cairns • Australia
9-12 July, 2007

14th International Congress on Sound & Vibration

AN INVESTIGATION ON THE SENSOR PROXIMITY EFFECT IN THE BEM–BASED NAH

Agustinus Oey[1], Jeong-Guon Ih[1], Hae-Won Jang[1], and Bong-Ki Kim[2]

[1]Center for Noise and Vibration (NoViC), Department of Mechanical Engineering
Korea Advanced Institute of Science and Technology (KAIST), Daejeon 305-701, Korea
[2]Korea Institute of Machinery and Materials (KIMM)
oeyaugust@gmail.com

Abstract

Near-field acoustical holography (NAH) using the boundary element method (BEM) is known to be very powerful in the source identification and visualization of many practical vibro-acoustic sources having irregular boundaries. In order to get rich information on the radiated wave components, both of propagating and evanescent waves, sensors should be positioned as close as possible to the source surface in principle. Therefore, it is beneficial to utilize a conformal hologram plane to the source surface; however, the usual way to measure the field data radiated from an irregular shaped source is to adopt a regular hologram plane in many cases for measurement ease. In such circumstances, the distance between sensors and the nearest point of the source surface cannot be maintained same for all measurement points in general. Consequently, different degree of information on propagating and non-propagating wave components will be detected by sensors at different positions. In this work, a preliminary theoretical and experimental investigations were conducted on such sensor proximity effect to the reconstruction errors in using the BEM–based NAH for interior problem.

1. INTRODUCTION

The technique of NAH has been shown to be effective in reconstructing the surface vibro-acoustic parameters as a backward problem as well as predicting the acoustic parameters of the radiated sound field using the restored source data as a forward problem. The quality of such parameter identification and calculation depends on the completeness of information, which should be experimentally given on the hologram plane. Accordingly, the selection of position and shape of the hologram plane and the arrangement of sensors over the hologram plane are very important issues in the implementation of NAH.

In general, hologram must be recorded sufficiently close to the source surface so that the evanescent wave information falls within the dynamic range of the sensor [1]. However, the usual BEM–based NAH has a hyper-singularity in the close near-field of the source surface. This problem can be alleviated with the use of nonsingular or weakly singular boundary integral formulation [2, 3]. Sensor and position mismatch are also very common to happen in the measurement process. A study on reconstruction errors as a result of inaccurate measurement positioning of sensors in planar acoustic holography was reported [4].

Another potential cause of error, as studied in this paper, is the disparity in information on propagating and non-propagating wave components captured by sensor due to the variation of the distance between sensor and the nearest point on source surface. The amount of error produced by a hologram with unequal distance distribution is larger than the one given by the conformal hologram located at average distance. Therefore, it is important to understand the nature of such kind of sensor proximity error because the arrangement of the hologram plane to be perfectly conformal is not practical for most of actual sources having irregular shapes.

2. SUMMARY OF THE BASIC THEORY OF BEM–BASED NAH

2.1 Inverse Formulation

If the boundary surface can be discretized into a number sufficiently small elements to be considered moving together as a unit in the domain of interest having surface S, then the Kirchhoff–Helmholtz integral equation can be presented in a discrete from as follows [5]:

$$[D]_S\{p\}_S = [M]_S\{v_n\}_S\,,\;\; \{p\}_f = [D]_f\{p\}_S + [M]_f\{v_n\}_S\,. \tag{1,2}$$

Here, $[D]_S$, $[M]_S$ are dipole and monopole matrices on the surface, $[D]_f$, $[M]_f$ are those corresponding to field pressures, and $\{p\}_f$, $\{v_n\}_S$ denote the field pressure vector and normal surface velocity, respectively. By substituting Eq. (1) into (2) and assuming the inverse of $[D]_S$ exists, the surface normal velocities can be obtained as

$$\{v_n\}_S = [G]_v^{\,+}\{p\}_f\,, \tag{3}$$

where $(\cdot)^+$ denotes the pseudo–inverse operator and $[G]_v \left(=[M]_f + [D]_f[D]_S^{-1}[M]_S\right)$ is the transfer matrix relating normal surface velocity to field pressures. By virtue of singular value decomposition (SVD), the normal surface velocity can be estimated as

$$\{\hat{v}_n\}_S = [W]_v[\Lambda^{-1}]_v[U]_v^H\{p\}_f\,, \tag{4}$$

where $[\Lambda]$ denotes a diagonal matrix whose diagonal elements are non–zero singular values and $[W]$ and $[U]$ are orthonormal matrices containing left and right singular vectors, respectively.

2.2 Regularization and Reconstruction Error

The solution given in Eq. (4) inherits an ill-posed inverse problem due to a small cluster of singular values in transfer matrix $[G]_v$ that its inverse includes a strong amplification of very small signal components at higher frequencies. Consequently, it becomes very sensitive to the noise and errors in the measured data. To resolve this problem, regularization techniques have been developed to refine the reconstruction image to an acceptable level [for example, 5–8]. In this study, the Tikhonov regularization technique was employed, for which the regularization parameter α was determined by the Generalised Cross Validation (GCV) method [9].

If the measurement noise $\{n\}$ coexists with the true signal and it is assumed as uncorrelated Gaussian random type having zero mean and variance σ^2, the expected squared value of reconstruction error is given by

$$E[(\{\hat{v}_n\}_S - \{v_n\}_S)^H (\{\hat{v}_n\}_S - \{v_n\}_S)] = \sigma^2 tr[[G]_v^H [G]_v]^{-1} \equiv \sigma^2 S_F\,, \tag{5}$$

where S_F represents singularity factor that indicates the degree of singularity of $[G]_v$. In other words, the reconstruction error is in proportion to the measurement noise variance and singularity factor of transfer matrix.

3. EXPERIMENT

A parallelepiped box having dimensions of 0.5 m (w) x 0.5 m (h) x 1.5 m (l) was constructed to test an interior problem. Figure 1 shows the boundary element model comprised of 726 linear triangular elements and 365 nodes having the characteristic length of 0.143 m. Based on the $\lambda/6$–criterion, the high frequency limit of interest was about 400 Hz. The first three cavity resonance frequencies were 114.3 Hz, 228.7 Hz, and 343 Hz.

All walls except the vibrating plate clamped at one end of the box were assumed rigid. The plate was made by 1 mm–thick steel sheet with size of 0.5 m x 0.5 m and was excited by an electro-dynamic shaker (B&K4809) at (0, 0.115, 0.105) point. Force transducer (Endevco 2312) and accelerometers (PCB 353B16) were used to measure the excitation force and the normal surface velocities at 49 evenly spaced points located on the vibrating plane, respectively.

Without loss of the nature of the system, a leaning hologram was chosen to simply simulate a diversity of source–field distances along the ***x***–direction. Figure 1 illustrates the measurement configuration, in which the leaning hologram plane is shown in the upper right side. The test was conducted for two cases representing different degree of distance inequality. Field pressures were measured at 49 evenly distributed positions using ¼–inch microphones (B&K 4935). In the first case (case 1), the maximum distance was 0.09 m, while the second one (case 2), 0.18 m. The distance difference in *x*–direction between the lower and the upper side of the leaning hologram were 0.06 m, for case 1, and 0.15 m, for case 2. Thus such arrangement defines the average distance for both cases at 0.06 m and 0.105 m, respectively.

For the comparison purpose, the pressure field over three flat holograms located at minimum, average, and maximum distances were also measured in a similar manner. The minimum distance was chosen as 0.03 m, which was larger than 20% of the element characteristic length, which avoids the singularity problem in the close near-field [2].

4. ANALYSIS OF RECONSTRUCTED RESULT

In the BEM–based NAH, transfer matrix $[G]_v$ depends solely on the geometrical condition of the problem. Transfer matrices for leaning and flat holograms were obtained and used for the calculation of singularity factor for the BEM models. Figure 2 shows the singularity factor calculated from Eq. (5) for cases 1 and 2, which shows typical decreasing trend as the increase of frequency. The high frequency excitation yields smaller singularity factor than the low frequency due to the fact that the non–radiating higher modes are more strongly excited than the low frequency excitation.

It is obvious to expect a high singularity factor when the distance between sensors and the nearest point on the source surface is either too far or not conformal to the source surface. This condition can be interpreted numerically as the linearly dependence between columns in the transfer function $[G]_v$, or, physically, can be translated as the lack of completeness in the information captured by sensors, which is closely related to the acoustical and geometrical characteristics of the fields at measurement points.

In Fig. 2, the singularity factor calculated from the leaning holograms plane is higher than that from the flat hologram plane located at an average distance. It indicates that the reconstructed surface normal velocity will be affected by the measured field pressure near the source points. In the viewpoint of reconstruction error, field points farther than the average distance influence the result dominantly, even though the field points which are closer to the source than the average distance contain significantly rich information on the source activity. Consequently, the reconstruction error using the hologram plane having different distances from the source, depending on the source position, would have larger reconstruction error than the conformal hologram plane located at an average distance.

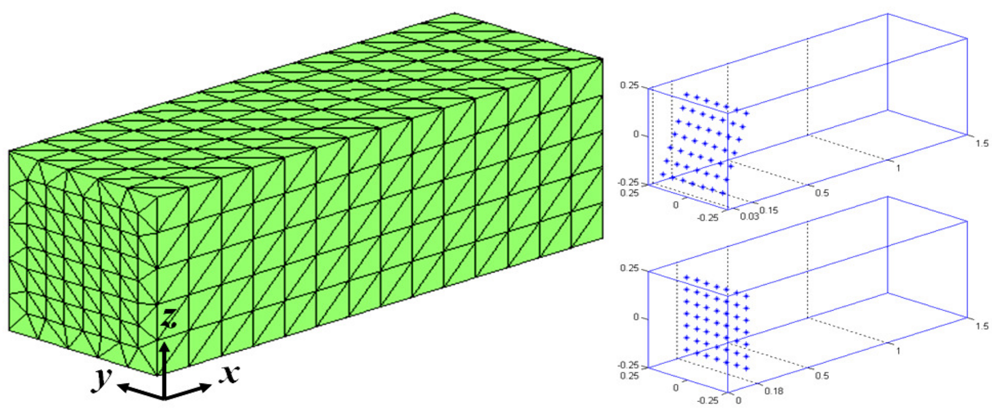

Figure 1. The BEM model of a parallelepiped box and holograms used in the experiment, in which the vibrating plate was defined on the left side of the box that has densely populated elements compared to the other areas. Both of leaning and flat holograms, has 7 by 7 evenly spaced measurement points.

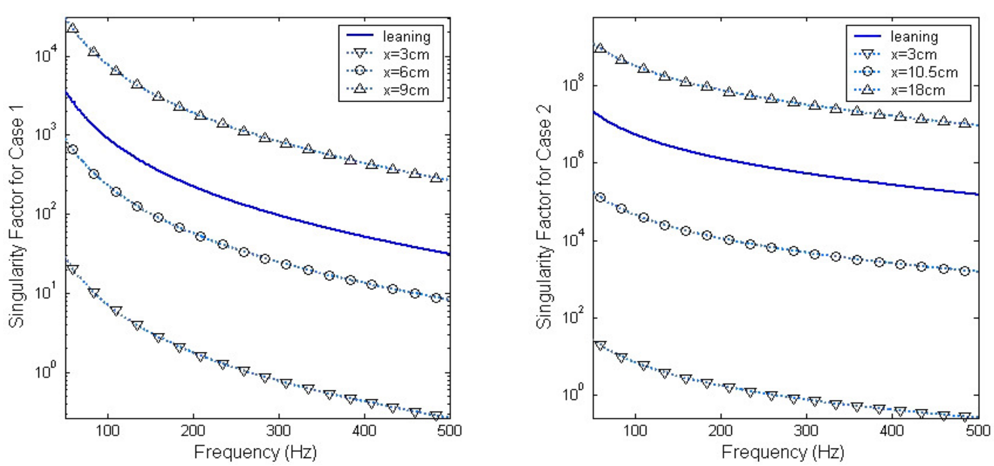

Figure 2. Singularity factors at the leaning holograms are typically higher than the one given by the flat hologram at average distance that signifies a higher reconstruction error.

4.1 Measured Hologram Data

Figures 3 and 4 present the measured field pressures at 97 Hz and 158 Hz on the flat and leaning holograms. These frequencies correspond to (2,2) and (2,3) modes of the vibrating plate. One can observe that the field pressures measured from the leaning holograms give a somewhat degraded information on the plate mode shape compared to the flat one. Also, one can find that the phase image, which is very critical for the reconstruction process, became a blurred one. It is noted that the field image became flattened in the upper side of the box, at which the distance between sensor and the nearest point on the vibrating surface became large. This is due to the fact that the high order evanescent wave vectors were diminished more than the nearest side. Because the decay rate of such non propagating components become fast as the frequency becomes high, the quality of pressure image at 158 Hz is worse than 97 Hz.

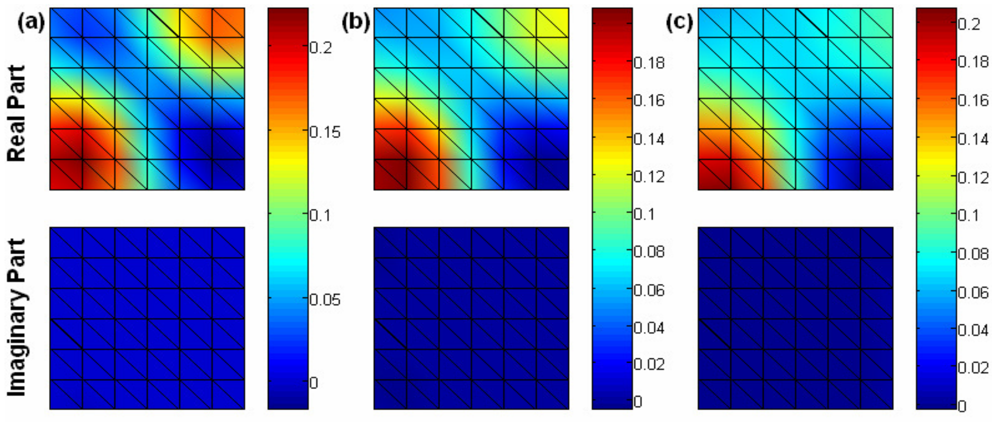

Figure 3. Field pressure images at 97 Hz: (a) over the flat hologram plane, (b) over the leaning hologram plane of case 1, (c) over the leaning hologram plane of case 2.

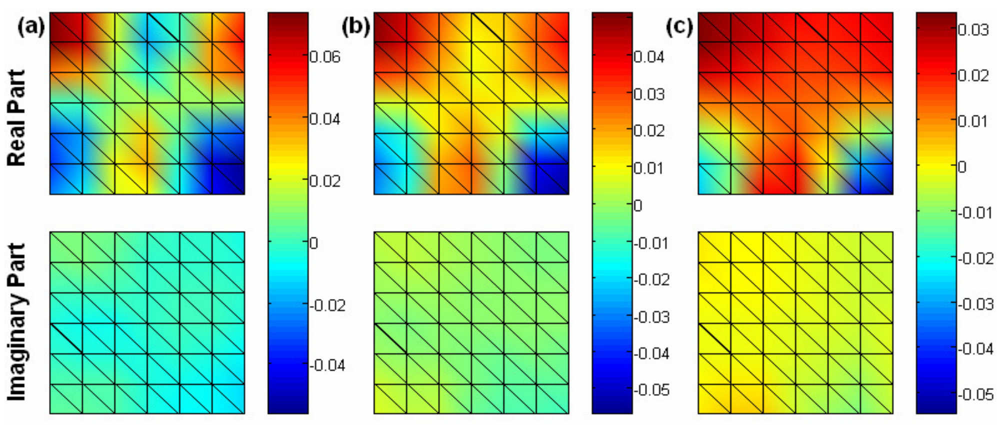

Figure 4. Field pressure images at 158 Hz: (a) over the flat hologram plane, (b) over the leaning hologram plane of case 1, (c) over the leaning hologram plane of case 2.

4.2 Surface Reconstruction

From the measured field pressure, the plate surface normal velocity was directly reconstructed using Eq. (3). Figures 5 and 6 present the measured and the reconstructed surface normal velocities given by holograms of case 1 and 2 at 97 Hz and 158 Hz. As we expected, conformal flat hologram in the close near field (all points at shortest distance) yielded better results compared to the leaning holograms. These figures confirm the reconstructed surface velocities were more affected by the measurement result in the hologram area farther than the average sensor–source distance, even though the quality of field pressure given by the closer hologram area is good. In order to investigate the reconstruction error given by a different degree of conformity, we have changed the slope of leaning holograms in the simulation.

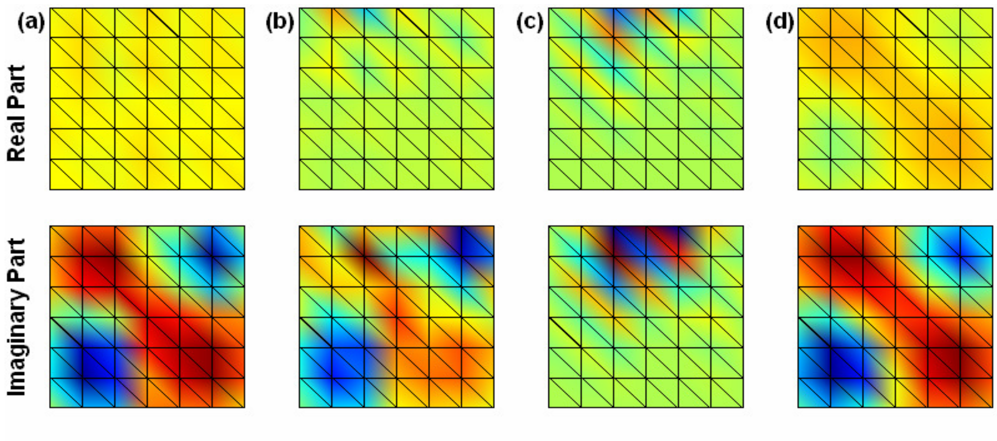

Figure 5. Normalized surface velocity distribution corresponding to (2,2) vibration mode reconstructed without regularization. Reconstructions were made from: (a) flat hologram, (b) leaning hologram plane (Case 1), (c) leaning hologram plane (Case 2). Measured normal velocity is shown in (d).

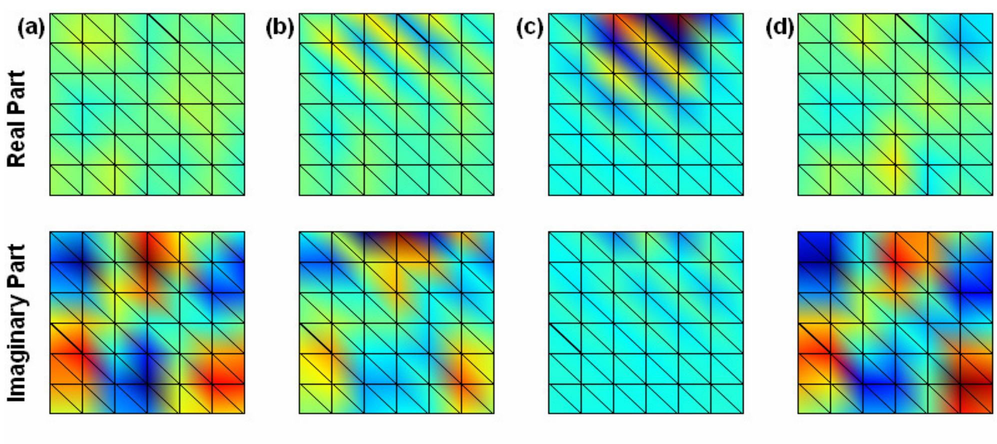

Figure 6. Normalized surface velocity distribution corresponding to (2,3) vibration mode reconstructed without regularization. Reconstructions were made from: (a) flat hologram, (b) leaning hologram plane (Case 1), (c) leaning hologram plane (Case 2). Measured normal velocity is shown in (d).

In the simulation, eight holograms having different slopes between 4.6^{o} to 32.6^{o} were tested for 50-400 Hz span. By defining θ as the leaning angle, the singularity factor for 8 leaning holograms were calculated and plotted in Fig. 7(a) as a function of $k\theta$. One can see that the singularity factor is affected by the average sensor-to-source distance. The singularity factor was amplified approximately by a factor of 10^4 by tripling the average sensor-to-source distance. Even though the measurement at the nearest positions along x=0.03 lead to a similar field pressure information, the corresponding singularity factor increases with $k\theta$, which suggests an dependency between distance and leaning angle.

Figure 7(b) shows the surface reconstruction error before regularization for leaning holograms of cases 1 and 2. The error percentage that was used in the figure and table is defined by L2 norm as

$$e = \left\| \{v_n\}_S - \{\tilde{v}_n\}_S \right\|_2 \Big/ \left\| \{v_n\}_S \right\|_2 \times 100\ (\%) \tag{6}$$

The blue solid curves denote the reconstruction errors calculated from the measurement, while the red dashed curves are errors calculated from the simulation. In the experiment, the signal-to-noise ratio (SNR) during the measurement was about 30 dB. However, as shown here, the reconstruction error for leaning holograms provided by the measurement was comparable to the simulation result with a SNR of about 10 dB. This is consistent with the fact that the amplitudes of non–propagating waves beyond the very close near field region become small, which are comparable magnitude with measurement noise.

Measured and calculated reconstruction errors have a similar tendency as can be seen in Fig. 7(b). At low frequencies and small leaning angles, the simulated reconstruction error is relatively higher than the measured one; contrastingly, at high frequencies and large leaning angles, the simulated has lower reconstruction error than the measurement result. One explanation is that the additive noise given in the simulation is normally distributed for all frequency range of interest; however, in the experiment, the measurement noise can takes different distribution. Because the phase information at low frequencies is simple and robust to noise, the disruption given by noise at high frequencies is likely to contribute to error in major. Figure 8 illustrates the effect of noise on the measured field pressures at 97 Hz and 158 Hz. The second reason is that the magnitudes of evanescent waves at high frequencies decay rapidly and easily falls to a level comparable to the measurement noise.

As mentioned before, the reconstruction field of the surface velocity is sensitive to the measurement noise; the regularization method can be utilized to improve the reconstruction result. Table 1 summarizes the calculated error percentage before and after regularization employing the Tikhonov regularization technique and GCV parameter finding method.

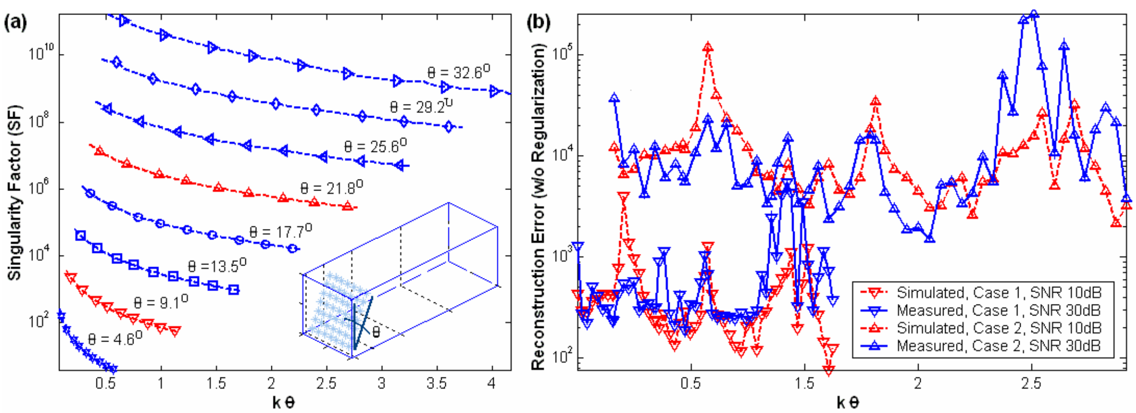

Figure 7. (a) Singularity factors calculated for 8 leaning holograms, (b) a comparison of measured and calculated reconstruction error for the selected cases.

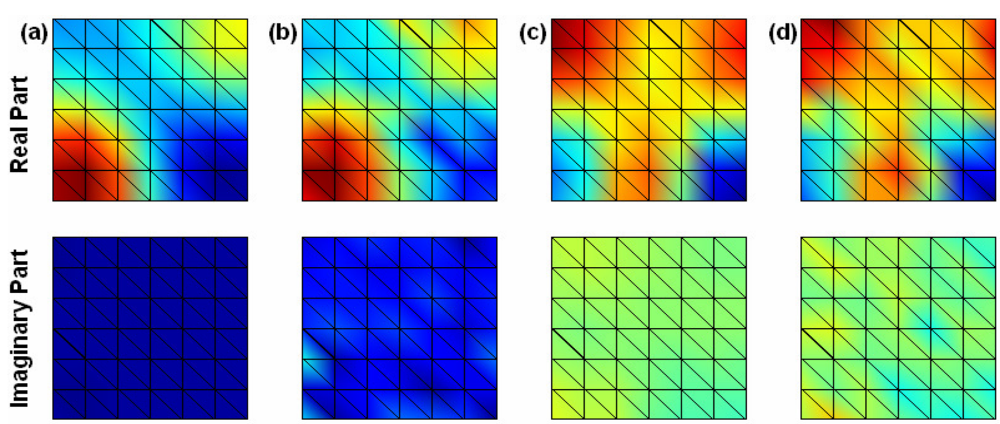

Figure 8. The field pressures provided by leaning hologram of case 1 at 97 Hz: (a) before and (b) after the addition of noise. Similar data for 158 Hz: (c) before and (d) after the addition of noise. The given signal-to-noise ratio was 10dB.

Table 1. Reconstruction errors of the surface velocity at the vibrating surface.

Test case	Frequency (Hz)	Reconstruction error (%)		
		Without regularization	With regularization	Reconstruction from a flat hologram plane at 0.03 m with regularization
1	97	320	43.6	30.7
	158	470	46.6	40.3
2	97	935	51.4	30.7
	158	1200	55.8	40.3

5. CONCLUSION

In this paper, a preliminary investigation result was reported on the effect of variation of sensor proximity to the source surface in implementing the BEM–based NAH. It was shown that the reconstruction error of source velocity is mostly affected by the field pressure at the positions located far from the source surface and the quality of reconstructed source image is affected largely from the nearest field data. It is thought that a further study should be directed to develop a method to compensate the error caused by different distances of sensors from the practical source surface.

ACKNOWLEDGEMENTS

This work was partially supported by BK21 Project.

REFERENCES

[1] E. G. Williams and J. D. Maynard, "Holographic imaging without the wavelength resolution limit", *Physical Review Letters* **45**, 554-557 (1980).

[2] B.-U. Koo, B.-C. Lee, and J.-G. Ih, "A non–singular boundary integral equation for acoustic problems", *Journal of Sound and Vibration* **192**, 263-279 (1996).

[3] S.-C. Kang and J.-G. Ih, "Use of non–singular boundary integral formulation for reducing errors due to near–field measurements in the boundary element method based near–field acoustic holography", *Journal of the Acoustical Society of America* **109**, 1320-1328 (2001).

[4] K.-U. Nam and Y.-H. Kim, "Errors due to sensor and position mismatch in planar acoustic holography", *Journal of the Acoustical Society of America* **106**, 1655-1665 (1999).

[5] B.-K. Kim and J.-G. Ih, "On the reconstruction of the vibro-acoustic field over the surface enclosing an interior space using the boundary element method", *Journal of the Acoustical Society of America* **100**, 3003-3016 (1996).

[6] B.-K. Kim and J.-G. Ih, "Design of an optimal wave-vector filter for enhancing the resolution of reconstructed source field by near-field acoustical holography (NAH)", *Journal of the Acoustical Society of America* **107**, 3289-3297 (2000).

[7] E. G. Williams, "Regularization methods for near–field acoustical holography", *Journal of the Acoustical Society of America* **110**, 1976-1988 (2001).

[8] Y. Kim and P. A. Nelson, "Optimal regularization for acoustic source reconstruction by inverse methods", *Journal of Sound and Vibration* **275**, 463-487 (2004).

[9] P. A. Nelson and S. H. Yoon, "Estimation of acoustic source strength by inverse methods: Part I, conditioning of the inverse problem," *Journal of Sound and Vibration* **233**, 643–668 (2000).